Western South Atlantic Holocene and Glacial Deepwater Hydrography derived from Benthic Foraminiferal Cd/Ca and Stable Carbon Isotope Data

By

Michael Horowitz

B.S., University of Massachusetts, 1994

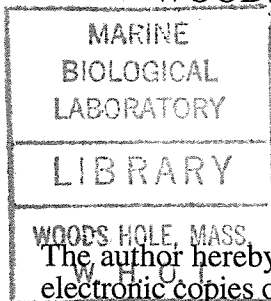Submitted in partial fulfillment of the requirements of the degree of

Master of Science

at the

MASSACHUSETTS INSTITUTE OF TECHNOLOGY

and the

WOODS HOLE OCEANOGRAPHIC INSTITUTION

January 1999

The author hereby grants to MIT and WHOI permission to reproduce paper and electronic copies of this thesis in whole or in part and to distribute them publicly.

Signature of Author _____

Joint Program in Oceanography,
Massachusetts Institute of Technology
and Woods Hole Oceanographic Institution
January 1999

Certified by _____ _____

Delia W. Oppo
Thesis Supervisor

Accepted by _____ _____

Deborah K. Smith
Chair, Joint Committee for Marine Geology and Geophysics
Massachusetts Institute of Technology/
Woods Hole Oceanographic Institution

WESTERN SOUTH ATLANTIC HOLOCENE AND GLACIAL DEEPWATER HYDROGRAPHY DERIVED FROM BENTHIC FORAMINIFERAL Cd/Ca AND STABLE CARBON ISOTOPE DATA

By
Michael Horowitz

Submitted to the Department of Earth, Atmospheric, and Planetary Sciences, at the Massachusetts Institute of Technology and to the Department of Marine Geology and Geophysics, at the Woods Hole Oceanographic Institution in January, 1999, in partial fulfillment of the requirements for the degree of Master of Science

ABSTRACT

Today, deep waters produced in the North Atlantic are exported through the western South Atlantic. Antarctic intermediate water (AAIW) also enters the Atlantic in this region. Circumpolar deep water (CDW) fills the depths below AAIW and above and below northern source waters. A depth transect of cores from 1567-3909 m water depth in the western South Atlantic are ideally located to monitor inter-ocean exchange of deep water, and variations in the relative strength of northern versus southern source water production. Last glacial maximum (LGM) Cd/Ca and $\delta^{13}C$ data indicate a nutrient-depleted intermediate-depth water mass. In the mid-depth western South Atlantic, a simple conversion of LGM $\delta^{13}C$ data suggests significantly less nutrient enrichment than LGM Cd/Ca ratios, but Cd/Ca and $\delta^{13}C$ data can be reconciled when plotted in CdW/$\delta^{13}C$ space. Paired LGM Cd/Ca and $\delta^{13}C$ data from mid-depth cores suggest increasingly nutrient rich waters below 2000 m, but do not require an increase in Southern Ocean water contribution relative to today. Cd/Ca data suggest no glacial-interglacial change in the hydrography of the deepest waters of the region. To maintain relatively low Cd/Ca ratios (low nutrients) in the deepest western South Atlantic waters, and in CDW in general, during the LGM requires an increased supply of nutrient-depleted glacial North Atlantic intermediate water (GNAIW) and/or nutrient-depleted glacial Subantarctic surface waters to CDW to balance reduced NADW contribution to CDW. LGM Cd/Ca and $\delta^{13}C$ data suggest strong GNAIW influence in the western South Atlantic which in turn implies export of GNAIW from the Atlantic, and entrainment of GNAIW into the Antarctic Circumpolar current.

Thesis Supervisor: Dr. Delia W. Oppo
Title: Associate Scientist in Marine Geology and Geophysics

TABLE OF CONTENTS

INTRODUCTION

Glacial-interglacial changes in deepwater hydrography of the North Atlantic region have been investigated using benthic foraminiferal Cd/Ca and $\delta^{13}C$ data to reconstruct past nutrient distributions. During the LGM, production of the relatively dense, nutrient-depleted NADW, which today fills most of the North Atlantic deeper than 1 km was curtailed. Below 2 km in the Atlantic, NADW was replaced by nutrient-rich waters, perhaps of southern origin (e.g. Boyle and Keigwin, 1982; Boyle and Keigwin, 1987; Oppo and Fairbanks, 1987; Duplessy et al., 1988; Curry et al., 1988; Charles and Fairbanks, 1992; Oppo and Lehmann 1993). These nutrient rich waters were overlain by the glacial analog of NADW, nutrient-depleted glacial North Atlantic intermediate water (GNAIW) (Boyle and Keigwin 1987; Duplessy et al., 1988; Curry et al., 1988; Boyle, 1992; Oppo and Lehmann, 1993). The glacial hydrography of the South Atlantic is less well understood.

Today, NADW flows through the western South Atlantic (Reid et al., 1977) into the Antarctic Circumpolar Current (ACC) transferring deepwater from the Atlantic into the Indian and Pacific (e.g. Broecker et al., 1985). Benthic foraminiferal Cd/Ca and $\delta^{13}C$, records suggest reduced contribution of nutrient depleted NADW to waters in the South Atlantic (Boyle, 1984; Boyle, 1992; Curry and Lohmann, 1982). During the LGM, $^{231}Pa/^{230}Th$ data imply continued vigorous export of North Atlantic water, consistent with an LGM global conveyor belt circulation in which GNAIW replaced NADW (Yu et al., 1996).

Here, we present Cd/Ca and $\delta^{13}C$ data from a depth-transect of cores to test the hypothesis that GNAIW penetrated far enough south to exit the Atlantic basin and enter the ACC. This is the first study which presents both benthic $\delta^{13}C$ and Cd/Ca data from South Atlantic cores shallower than ~2.5 km. The western South Atlantic is an ideal location to monitor N-S deepwater source variations and inter-ocean exchange of water, because the region is a conduit for northern source waters leaving the Atlantic, and AAIW entering the

Atlantic. Sites in the western South Atlantic should also be sensitive to variations in the relative strength of northern and southern deep water production, because NADW and AAIW flow through the region as western boundary currents and recirculated CDW fills the depths above and below NADW (Reid et al., 1977).

BACKGROUND:

The interplay of ocean circulation and biological redistribution of nutrients creates unique chemical signatures for northern and southern source deep waters. NADW has low nutrient concentrations while Southern Ocean Water (SOW) has high nutrient concentrations, mainly because of the disparity in surface water nutrient contents between regions of deep convection (e.g. Broecker et al., 1985). During construction of new biomass, primary producers fractionate carbon isotopes in favor of ^{12}C (e.g. Kroopnick, 1985) and incorporate P (Redfield, 1963) and Cd (Martin and Knauer, 1976). Once deep waters are isolated from the surface, nutrient contents increase as a result of remineralization of marine snow. As a result of the biological cycle of nutrient uptake in surface waters and remineralization at depth, P and $\delta^{13}C$ are inversely correlated (Kroopnick, 1985) and P and Cd are positively correlated (Boyle et al., 1976; Martin and Knauer, 1976; Knauer and Martin, 1981).

The temperature dependent fractionation which occurs during CO_2 exchange at the sea surface alters the $\delta^{13}C$ of DIC in surface waters (Mook, 1974), but does not affect nutrient concentrations. Gas exchange at colder temperatures results in higher $\delta^{13}C$ values than gas exchange at warmer temperatures. Because the time needed to reach isotopic equilibrium is longer than the residence time of most surface waters (Broecker and Peng 1982), the isotopic imprint of gas exchange is variable even at a given temperature. In areas where wind speeds are high, gas exchange rates are high, bringing the sea surface $\delta^{13}C$ values closer to isotopic equilibrium with the atmosphere (Liss and Merlivat, 1986; Broecker and Maier-Reimer, 1992). Because of the greater mobility of $^{12}CO_2$, the

direction of carbon dioxide flux also influences the air-sea exchange signature imparting a negative surface ocean air-sea exchange signature in regions of CO_2 invasion and positive exchange signature in regions of CO_2 evasion (Lynch-Stieglitz et al., 1995).

Foraminiferal shell chemistry can be used to reconstruct past ocean circulation (e.g. Curry et al., 1988; Duplessy et al. 1988; Boyle, 1988). Certain species of benthic foraminifera appear to record the $\delta^{13}C$ of bottom water dissolved inorganic carbon (DIC) (Belanger et al., 1981; Graham et al., 1981; Grossmann, 1984; Curry et al., 1988) and the [Cd] in sea water (Boyle, 1981, 1988). However, neither benthic foraminiferal Cd/Ca ratios nor carbon isotope data are influenced solely by water chemistry (Boyle, 1992; McCorkle et al., 1995; Elderfield et al., 1996; Zahn et al., 1986; Mackensen et al., 1993; Spero et al., 1991,1997). For example, recent studies suggest that the $\delta^{13}C$ values of the benthic foraminifera used to reconstruct past deepwater dissolved inorganic carbon (DIC) $\delta^{13}C$ values may be as much as ~0.5‰ lower than bottom water DIC $\delta^{13}C$ when overlying surface ocean productivity is high (Mackensen, et al., 1993), as may have been the case in many regions of the Southern Ocean previously studied. Furthermore, in contrast to $\delta^{13}C$ data, Cd/Ca ratios of benthic foraminifera from cores within deep Southern Ocean water suggest little or no glacial-interglacial nutrient change (Boyle, 1992; Oppo and Rosenthal, 1994; Rosenthal et al., 1997). The physiological bases of the extraneous influences on benthic foraminiferal chemistry are not fully understood, but correction for some influences other than water chemistry is routine. For example, Cd/Ca ratios of calcitic benthic foraminifera are converted to a quantity, CdW, which is an estimate of the cadmium concentration in seawater (Cd_w) using a depth dependent distribution coefficient (Boyle, 1992).

MATERIALS AND METHODS

Core sites and modern western South Atlantic hydrography and nutrient chemistry

The cores from the Brazilian Margin range in water depth from 1567 m to 3909 m and in latitude between approximately 32 deg. S and 26 deg. S (Table 1; Figure 1). The waters bathing core sites in the western South Atlantic are a mixture of up to three of the five water masses listed in Table 2. To assess the percentage of each of these water masses overlying sites, we have taken end-member properties for northern component water (NCW ~ NADW), and the deeper southern component water (SCW ~ LCDW) from Oppo and Fairbanks (1987) and Broecker et al. (1985). We have taken Labrador Sea Water (LSW) properties from Broecker and Peng (1982). We have also estimated an Upper Circumpolar Deepwater (UCDW) temperature from GEOSECS data and derived an AAIW end-member from GEOSECS data and measurements made by Kroopnick (1985)

The two deepest cores, RC16-85 (3909 m) and RC16-86 (3759 m) lie close to CDW in salinity vs. temperature space (Figure 2). The mid-depth cores, RC16-84 (2438 m) and V24-253 (2069 m) lie close to NADW and LSW, respectively. The shallowest core, RC16-119 (1567 m), is a mixture of LSW, UCDW, and AAIW.

Stratigraphy and nutrient proxies

Stable carbon and oxygen isotope records were generated using *Cibicidoides wuellerstorfi* in RC16-119, V24-253, and RC16-84 (Table 4). This species of foraminifera appears to record the $\delta^{13}C$ of bottom water DIC (Belanger et al., 1981; Graham et al., 1981; Grossmann, 1984; Curry et al., 1988). Due to very low benthic foraminiferal abundances in RC16-86 (3759 m) and RC16-85 (3909 m), stable oxygen isotope records were generated using *Globorotalia inflata* picked from the 250-300 μm size fraction (Table 4), and the benthic foraminifera were saved for trace element analysis.

Stable isotope measurements were made at the Woods Hole Oceanographic Institution (WHOI) on a Finnigan MAT 252 with automated kiel device which has 46

single-reaction chambers, 23 per each of two gas lines. Acid temperature was maintained at approximately 70°C. The standard deviation of the isotope values of the National Bureau of Standards (NBS) carbonate standard NBS-19 was 0.08‰ and 0.03‰ for $\delta^{18}O$ and $\delta^{13}C$ respectively. NBS-19 isotope values were used to calibrate to Pee Dee Belemnite ($\delta^{18}O$= -2.2 VPDB, $\delta^{13}C$=1.95 VPDB). Radiocarbon dates were measured at WHOI's AMS facility on 22 samples of either mixed planktonic foraminifera or *G. ruber* in the case of RC16-119 (Table 5).

Benthic foraminiferal Cd, Mn, and Ca analyses were made following the procedure of Boyle and Keigwin (1985/6) on a Hitachi Z8200 atomic absorption spectrophotometer (AAS) tandem flame and graphite furnace. Numerous species were used for Cd/Ca measurements (Table 6) because there appears to be little systematic offset between the Cd/Ca ratios of various calcitic benthic foraminiferal species (Boyle, 1988). Each sample consisting of between 1 and 20 individual specimen of benthic foraminifera was cleaned for trace metal analysis according to the procedure of Boyle and Keigwin (1985/6) with a reversal of the oxidative and reductive steps to improve the removal of authegenic Cd deposits on the outside of foraminiferal shells (Boyle et al., 1995; Rosenthal, 1994; Rosenthal et al., 1995). Mn/Ca ratios were used to assess the efficacy of the cleaning procedure. Samples with Mn/Ca ratios higher than 120 μmol/mol were rejected.

Three consistency standards were treated as samples in each run in order to assess the analytical precision of the measurements on the AAS. Boyle (1995) reported an RSD of 4.1 % for a consistency standard of 0.18 μmol/mol. The relative standard deviations (RSD) for our consistency standards are 8.23% for 0.13 μmol/mol (n=13), 8.34% for 0.09 μmol/mol (n=12), and 13.69% for 0.04 μmol/mol (n=12). High RSD values were largely due to an unrecognized problem with the photomultiplier.

RESULTS

Stratigraphy

Stratigraphy was developed for the cores using foraminiferal $\delta^{18}O$ values and 22 AMS radiocarbon dates. The glacial-interglacial ice-volume/temperature signal is evident in all the $\delta^{18}O$ records (Figure 3 and 4), but there are reversals in radiocarbon ages in RC16-84 and RC16-119. The age reversals do not compromise our conclusions, because the reversed dates are either on Termination I (RC16-119) or are both glacial (RC16-84), and we focus on Cd/Ca and $\delta^{13}C$ differences between the LGM and the Holocene (Figure 5 and 6).

Nutrient proxies

The Cd/Ca and $\delta^{13}C$ data used to reconstruct Holocene and LGM depth transects are circled (Figure 4). The data chosen for the Holocene transect are from the core top and near core top. Data for the LGM transect were selected on the basis of maximum $\delta^{18}O$ values and radiocarbon ages between 15 and 20 kyr.

Holocene *C. wuellerstorfi* $\delta^{13}C$ values of ~1.1‰ between 1500 m and 2500 m are 0.3‰-0.4‰ higher than $\delta^{13}C$ values from the nearest GEOSECS station (Figure 7). We used a depth-dependent distribution coefficient (Boyle, 1992) and assumed a constant seawater Ca concentration of 0.01 mol/kg to convert calcitic benthic foraminiferal Cd/Ca values to a foraminiferal estimate (CdW) of the Cd concentration in sea water (Cd_w) (Boyle, 1992). For *Hoeglundina elegans*, we have used a distribution coefficient of 1.0 (Boyle et al., 1995). CdW values were converted to estimates of phosphate using the relationship for phosphate concentrations higher than ~ 1.3 μmol/kg (Boyle, 1988). Holocene Cd/Ca ratios match GEOSECS phosphate profiles reasonably well (Figure 6), perhaps slightly underestimating nutrient concentrations between 2000 and 3000 m water depth.

9

Downcore Cd/Ca and $\delta^{13}C$ data suggest similar patterns of nutrient change, with glacial nutrient depletion in the shallowest core (RC16-119, 1567 m), and glacial nutrient enrichment in the mid-depth cores (V24-253, 2069 m; RC16-84, 2438 m). Cd/Ca data suggest no change in the deepest core (RC16-85, 3909 m) where no $\delta^{13}C$ data is available (Figure 5; Table 7).

After adjusting glacial $\delta^{13}C$ values for glacial-interglacial mean ocean increase of 0.3 ‰ (Shackleton 1977; Curry et al., 1988; Duplessy et al., 1988), glacial-interglacial differences in $\delta^{13}C$ values (Table 7) were converted to rough estimates of phosphate change with a conversion factor of $1.1*\Delta phosphate = \delta^{13}C_{G-I}$ (Broecker and Maier-Reimer, 1992; Lynch-Stieglitz et al., 1995). This conversion does not account for glacial-interglacial variations in air-sea exchange signature, average $\delta^{13}C$ values of organic matter, or mean ocean ΣCO_2. Because there apparently was a negligible glacial-interglacial Cd change (Boyle, 1988, 1992), there was no correction to the phosphate difference between glacial and interglacial times estimated from Cd/Ca data (Table 7). Later, the differences between LGM Cd/Ca and $\delta^{13}C$ data will be used to constrain glacial circulation.

DISCUSSION

Glacial-interglacial Cd/Ca and $\delta^{13}C$ contrasts from mid-depth and deep cores are consistent with published data from the South Atlantic (Curry and Lohmann, 1982; Boyle, 1984; Oppo and Fairbanks, 1987; Boyle 1992; Rosenthal et al., 1997; Ninnemann and Charles, 1997). Addition of our data from the shallower cores suggests that during the LGM, a nutrient depleted watermass above 2 km overlay nutrient-rich waters (Figure 5; Figure 6b).

In order to best use Cd/Ca and $\delta^{13}C$ data, we follow the lead of Lynch-Steiglitz et al. (1996) and plot $\delta^{13}C$ vs. CdW (Figures 8, 9 and 10). On the CdW/$\delta^{13}C$ diagrams, mixing between northern source water and southern source water moves data parallel to

mixing lines between the end-members. Watermass aging and organic matter remineralization cause data to move along lines of "Redfield" ratio organic matter remineralization (Broecker and Maier-Reimer, 1992; Lynch-Steiglitz et al., 1995, 1996). For the glacial CdW/δ^{13}C diagram, these lines assume a 0.3‰ lower mean ocean δ^{13}C (Duplessy et al., 1988), a 2‰ higher average organic matter δ^{13}C (Lynch-Steiglitz et al., 1995, 1996), a 4% increase in total inorganic carbon, and no change in the oceanic inventory of Cd during the LGM (Boyle, 1988; Boyle, 1992; Rosenthal et al., 1995). Redfield ratio organic matter remineralization lines also can be thought of as defining lines of equal gas exchange signature ($\delta^{13}C_{as}$). The $\delta^{13}C_{as}$ equations we use are: $\delta^{13}C_{as} = \delta^{13}C_{meas} + 2.75*Cd_w - 2.0$ for the Holocene, and $\delta^{13}C_{as} = \delta^{13}C_{meas} + 2.375*Cd_w - 1.46$ for the LGM (see Lynch-Stieglitz et al., 1995, 1996 for an in depth discussion). The lines on Figures 8, 9 and 10 have arbitrarily been plotted at $\delta^{13}C_{as}$ equal to 1, 0, and -1. To estimate northern versus southern end-member composition on the CdW/δ^{13}C diagram, data should be backtracked along lines of Redfield ratio organic matter remineralization to the mixing line between end-members. Holocene end-member compositions (Figure 8) are derived from conversion of GEOSECS phosphate to CdW values using the global CdW phosphate regression of Boyle (1988). GNAIW, glacial SOW and deep Tropical Pacific end-members (Figures 9 and 10) are derived from Boyle (1992). The glacial Subantarctic surface water point is derived from planktonic foraminiferal δ^{13}C (Ninnemann and Charles, 1997) and Cd/Ca measurements (Rosenthal et al., 1997; Rickaby and Elderfield, submitted manuscript, 1998). The distribution coefficient for planktonic foraminifera was taken from Mashiotta and Lea (1997), and based on LGM SSTs at RC11-120 (Hayes et al., 1976) is also consistent with temperature dependant estimates of planktonic distribution coefficients (Rickaby and Elderfield, submitted manuscript, 1998).

Core top foraminiferal δ^{13}C values are roughly 0.3‰-0.4‰ higher than δ^{13}C values from the nearest GEOSECS station (Figure 7). *C. wuellerstorfi* δ^{13}C values ~0.2‰ higher than bottom water have been documented in intermediate and mid-depth

cores (McCorkle et al., 1995). This is the first time that a positive offset as large as ~0.4‰ has been documented.

Missing core top material might explain the offset of our foraminiferal data from Kroopnick's (1985) $\delta^{13}C$ values (Figure 7), and from GEOSECS phosphate values (Figure 6), as well as the disagreement of watermass percentages predicted by temperature and salinity (Reid et al., 1977; Figure 2) versus CdW and $\delta^{13}C$ (Table 8; Figure 8) for RC16-119 (1567 m). A possible explanation for slightly low core-top CdW values would be that during this earlier period (~3-5 kyr before the present according to radiocarbon ages), NADW production was stronger and may have penetrated further south than today. Good agreement between watermass compositions estimated by modern salinity versus temperature and by core-top CdW versus $\delta^{13}C$ values, but lesser aging implied by foraminiferal proxies than by bottom water $\delta^{13}C$ and P supports the possibility of stronger NADW production during this earlier Holocene period. In our core-top data, high $\delta^{13}C$ values relative to CdW values could be a result of a more positive gas exchange signature for any or all end-members during this period. Alternatively, the offsets from modern watermass properties could be a result of foraminiferal "vital" effects.

LGM $\delta^{13}C$ and Cd/Ca data (Figure 5 and 6) demonstrate that intermediate waters of the western South Atlantic were nutrient-depleted during the LGM. Waters from the western South Atlantic fall along a line of organic matter remineralization associated with GNAIW which has a much higher preformed $\delta^{13}C$ value than glacial Southern Ocean water (Figure 9). Thus, the glacial CdW/$\delta^{13}C$ data suggest that GNAIW is the most likely source of nutrient depleted water bathing RC16-119 (Figure 9). In CdW/$\delta^{13}C$ space, RC16-119 (1567 m) in particular falls very close to GNAIW, but more than 1‰ away from Subantarctic surface waters in $\delta^{13}C$ (Ninnemann and Charles, 1997), suggesting GNAIW is the source of water bathing this site (Figure 9). The presence of GNAIW at 28S provides evidence to support the hypothesis of a glacial conveyor belt circulation in which NADW was replaced by GNAIW (Yu et al., 1996).

On the CdW/δ^{13}C diagram (Figure 9), mid-depth western South Atlantic data (2069 and 2438 m) fall along lines of equal gas exchange signature extending roughly from GNAIW also suggesting a predominantly northern source for waters bathing these sites during the LGM. Furthermore, western South Atlantic data also fall further to the right of the mixing line on the CdW/δ^{13}C diagram than similar depth North Atlantic data (~2100 m and 2400 m North Atlantic waters), implying southward flow and aging of mid-depth waters.

The Cd/Ca data from the two deepest cores confirm previous studies of cores from similar and deeper depths showing low amplitude glacial-Holocene change in LCDW (e.g. Boyle, 1992; Oppo and Rosenthal, 1994; Rosenthal et al., 1997), and contrast with δ^{13}C data from similar depths suggesting substantially greater glacial than Holocene nutrient levels (Oppo and Fairbanks, 1987; Charles and Fairbanks, 1992). Much of the earlier δ^{13}C data generated on South Atlantic cores comes from regions overlain by very productive surface waters, where high fluxes of low-δ^{13}C organic matter probably reduces the δ^{13}C value of the water just at the sediment-water interface where the foraminifera are living (e.g. Mackensen et al., 1993). Although these very low δ^{13}C values are probably lower than that of the surrounding bottom water, benthic δ^{13}C data generated from cores underlying relatively unproductive regions (Bickert and Wefer, 1996) continue to suggest a minimal δ^{13}C gradient between the deep Atlantic and deep Pacific, inconsistent with the Cd/Ca data if a simple δ^{13}C-phosphate relationship is used. Although it is difficult to imagine that a decrease in nutrient-depleted NADW, documented throughout the Atlantic basin with both δ^{13}C and Cd/Ca data (e.g. Boyle and Keigwin 1982; Boyle, 1984; Boyle and Keigwin,1987; Duplessy et al., 1988; Curry et al., 1988; Boyle, 1992; Bertram et al., 1995) would not affect nutrient levels in LCDW, reduced contribution of nutrient-depleted NADW to CDW could have been compensated for by an increased supply of GNAIW, which we now know extended to at least 28S. A reduced supply of nutrient-depleted NADW to CDW may also have been partially compensated by incorporation of

Subantarctic surface water, because Subantarctic Indian and Pacific planktonic and benthic Cd/Ca and $\delta^{13}C$ suggest glacial nutrient depletion in these surface waters (Rosenthal et al., 1997; Ninnemann and Charles, 1997). LGM benthic Cd/Ca data also suggest local sources of nutrient depleted deep water in the Indian sector of the Southern Ocean (Rosenthal et al., 1997). All of these scenarios could result in unchanged LCDW nutrient levels.

Additional important observations related to the LGM Cd/Ca-$\delta^{13}C$ data set can be derived from the CdW/$\delta^{13}C$ diagram. First, the CdW/$\delta^{13}C$ diagram suggests that most of the open North Atlantic data is a mixture of GNAIW and SOW, with varying degrees of aging (Figure 10). Second, the CdW/$\delta^{13}C$ diagram suggests that Subantarctic surface waters could be a partial source of deep Southern Ocean waters (Figure 9). This deduction is based on the observation that LGM Cd/Ca and $\delta^{13}C$ data from Southern Ocean cores (Boyle, 1992; Oppo and Rosenthal, 1994) fall roughly along the line of regeneration of organic matter (Broecker and Maier-Reimer, 1992; Lynch-Stieglitz et al., 1995) extending from Subantarctic Indian Ocean surface water (Ninnemann and Charles, 1997; Rosenthal et al., 1997; Rickaby and Elderfield, submitted manuscript, 1998). Third, the position of deep Tropical Pacific data (Boyle, 1992) on the the CdW/$\delta^{13}C$ diagram suggests that like today (Broecker et al., 1998), deep Tropical Pacific waters were an ~50/50 mixture of northern and southern source waters during the LGM. The amount of aging of deep Tropical Pacific waters implied by the CdW/$\delta^{13}C$ diagram is also similar to today, consistent with radiocarbon evidence (Broecker et al., 1990).

Thus, it is possible to arrive at an internally consistent LGM deepwater circulation using a CdW/$\delta^{13}C$ approach. Like today, deep Atlantic and Pacific waters were a mixture of North Atlantic and Southern Ocean sources with the differences in apparent nutrient concentrations accounted for by varying degrees of aging. Even though the glacial to interglacial change in the $\delta^{13}C$ of CDW seems large in comparison to the glacial to interglacial change Cd/Ca change, the fact that most of the combined glacial data can be described as an aged mixture of CDW and NCW suggests that the Cd/Ca-$\delta^{13}C$ debate

14

should refocus on the origin of the low CdW and $\delta^{13}C$ values found together in glacial Subantarctic surface waters, which probably supplied glacial CDW.

CONCLUSIONS

Core top Cd/Ca and $\delta^{13}C$ data suggest more nutrient depleted water masses bathing intermediate and mid-depth sites than suggested by modern water column measurements (GEOSECS expedition; Reid et al., 1977). Stronger NADW production earlier in the Holocene could explain the difference between phosphorus estimates based on core top Cd/Ca ratios and modern water column phosphate measurements. Stronger NADW production does not explain all of the discrepancy in $\delta^{13}C$ data, because the discrepancy between modern water column measurements and core top foraminiferal measurements is larger in $\delta^{13}C$ data than Cd/Ca data. A more positive gas exchange signature for any end-member earlier in the Holocene could explain modern-core top $\delta^{13}C$ offset not accounted for by Cd/Ca data. Alternatively, we cannot eliminate the possibility that high $\delta^{13}C$ values and low Cd/Ca ratios were caused by foraminiferal vital effects.

LGM South Atlantic Cd/Ca and $\delta^{13}C$ suggest a nutrient depleted water mass above about 2000 m and nutrient enriched water below that depth (Figures 5 and 6). Using a simple conversion of $\delta^{13}C$ data to phosphate suggests some discrepancies between LGM Cd/Ca and $\delta^{13}C$ data, but the data are internally consistent when viewed on a CdW/$\delta^{13}C$ diagram (Figures 9 and 10). Paired Cd/Ca and $\delta^{13}C$ data suggest that GNAIW extended to at least 28S during the LGM, and suggest a predominantly northern source of mid-depth waters. Cd/Ca ratios in the deepest western South Atlantic sites suggest no change in the nutrient content of LCDW.

The presence of GNAIW at 28S combined with little or no change in the nutrient content of LCDW provides supporting evidence for a global conveyor belt circulation in which NADW was replaced by GNAIW during the LGM (Yu et al., 1996). Glacial SOW

15

apparently originated in the Subantarctic, and deep Pacific waters were an ~50/50 mixture of northern and southern source waters like today.

REFERENCES

Belanger, P.E., W.B. Curry, and R.K. Matthews, Core top evaluation of benthic foraminiferal isotopic ratios for paleoceanographical interpretations, *Paleogeogr., Palaeoclimatol., Palaeoecol.*, 33, 205-221, 1981.

Bertram, C.J., H. Elderfield, J. MacDonald, and N.J. Shackleton, Cadmium/calcium and carbon isotope reconstructions of the glacial northeast Atlantic Ocean, *Paleoceanography*, 10, 643-660, 1995.

Bickert, T., and G. Wefer, Late Quaternary Deep Water Circulation in the South Atlantic: Reconstruction from Carbonate Dissolution and Benthic Stable Isotopes, in *The South Atlantic: Present and Past Circulation*, edited by G.Wefer, W.H. Berger, G. Siedler, and D.J. Webb, pp. 599-620, Springer-Verlag, Berlin, 1996.

Boyle, E.A., F.R. Sclater, and J.M. Edmond, On the marine geochemistry of cadmium, *Nature*, 263, 42-44, 1976.

Boyle, E.A., Cadmium, zinc,copper and barium in foraminifera tests, *Earth Planet. Sci. Lett.*, 53, 11-35, 1981.

Boyle, E.A. and L.D. Keigwin, Deep Circulation of the North Atlantic over the Last 200,000 Years: Geochemical Evidence, *Science*, 218, 784-787, 1982.

Boyle, E.A., Cadmium in benthic foraminifera and abyssal hydrography: Evidence for a 41 kyr obliquity cycle, In *Climate Processes and Climate Sensitivity*, J. Hansen and T. Takahashi eds., AGU, Geophysical Monograph 29, 360-368, 1984.

Boyle, E.A., and L.D. Keigwin, Comparison of Atlantic and Pacific paleochemical records for the last 215,000 years: changes in deep ocean circulation and chemical inventories, *Earth Planet. Sci. Lett.*, 76, 135-150, 1985/6.

Boyle, E.A., and L.D. Keigwin, North Atlantic thermohaline circulation during the past 20,000 years linked to high-latitude surface temperature, *Nature*, 330, 35-40, 1987

Boyle, E.A., Cadmium: Chemical Tracer of Deepwater Paleoceanography, *Paleoceanography*, *3* (4), 471-489, 1988.

Boyle, E.A., Cadmium and $\delta^{13}C$ paleochemical ocean distributions during the stage 2 glacial maximum, *Annu. Rev. Earth Planet. Sci.*, 20, 245-287, 1992.

Boyle, E.A., L. Labeyrie, and J.-C. Duplessy, Calcitic foraminiferal data confirmed by cadmium in aragonitic *Hoeglundina*: Application to the last glacial maximum in the northern Indian Ocean, *Paleoceanography*, 10, 881-900, 1995.

Broecker, W.S., and T.-H. Peng, *Tracers in the Sea*, 690 pp., Eldigio, Palisades, New York, 1982.

Broecker, W.S., T. Takahashi, and T. Takahashi, Sources and flow patterns of deep ocean waters as deduced from potential temperature, salinity, and initial phosphate concentration, *J. Geophys. Res.*, 90, 6925-6939, 1985.

Broecker, W.S., T.-H. Peng, S. Trumbore, G. Bonani, and W. Wolfli, The distribution of radiocarbon in the glacial ocean, *Global Biogeochem. Cycles*, 4, 103-117, 1990.

Broecker, W.S. and E. Maier-Reimer, The influence of air sea exchange on the carbon isotope distribution in the sea. *Global Biogeochem Cycles*, 6 (3), 315-320, 1992.

Charles, C.D., and R.G. Fairbanks, Evidence from Southern Ocean sediments for the effect of North Atlantic deep-water flux on climate, *Nature*, 355, 416-419, 1992.

Curry, W.B., and G.P. Lohmann, Carbon Isotopic Changes in Benthic Foraminifera from the Western South Atlantic: Reconstruction of Glacial Abyssal Circulation Patterns, *Quat. Res.*, 18, 218-235, 1982.

Curry, W. B., J. C. Duplessy, et al., Changes in the distribution of $\delta^{13}C$ of deep water ΣCO_2 between the last glaciation and the Holocene, *Paleoceanography 3*(3): 317-341, 1988.

Duplessy, J.C., N.J. Shackleton, R.G. Fairbanks, L. Labeyrie, D. Oppo, and N. Kallel, Deepwater Source Variations During the Last Climatic Cycle and their Impact on the Global Deepwater Circulation, *Paleoceanography*, 3(3), 343-360, 1988.

Elderfield, H., C.J. Bertram, and J. Erez, A biomineralization model for the incorporation of trace elements into foraminiferal calcium carbonate, *Earth Planet. Sci. Lett.*, 142, 409-423, 1996.

Graham, D.W., B. Corliss, M.L. Bender, and L.D. Keigwin, Carbon and oxygen isotopic disequilibria of recent deep-sea benthic foraminifera, *Mar. Micropaleontol.*, 6, 483-479, 1981.

Grossman, E.L. Stable isotope fractionation in live benthic foraminifera from the Southern California borderland, *Paleogeogr., Palaeoclimatol., Palaeoecol.*, 33, 301-327, 1981.

Hays, J.D., J. Imbrie, and N.J. Shackleton, Variations in the Earth's Orbit: Pacemaker of the Ice Ages, *Science*, 194, 1121-1131, 1976.

Knauer, G.A., and J.H. Martin, Phosphorus-cadmium cycling in northeast Pacific waters, *J. Mar. Res.*, 39, 65-76, 1981.

Kroopnick, P.M., The distribution of $\delta^{13}C$ of ΣCO_2 in the world oceans, *Deep-Sea Research*, *32* (1), 57-84, 1985.

Liss, P.S. and L. Merlivat, Air-sea gas exchange rates: Introduction and synthesis, in *The Role of Air-Sea Exchange in Geochemical Cycling*, edited by P. Buat-Menard, pp. 113-127, D. Reidel, Norwell, Mass., 1986.

Lynch-Stieglitz, J., T.F. Stocker, W.S. Broecker, and R.G. Broecker, The influence of air-sea exchange on the isotopic composition of oceanic carbon: Observation and modeling, *Global Biogeochemical Cycles*, 9, 653-665, 1995.

Lynch-Stieglitz, J., A. van Geen, and R.G. Fairbanks, Interocean exchange of Glacial North Atlantic Intermediate Water: Evidence from Subantarctic Cd/Ca and $\delta^{13}C$ measurements, *Paleoceanography, 11*(2), 191-201, 1996.

Mashiotta, T.A., D.W. Lea, and H.J. Spero, Experimental determination of cadmium uptake in shells of the planktonic foraminifera *Orbulina Universa* and *Globigerina bulloides*: Implications for surface water paleoreconstructions, *Geochim. Cosmochim. Acta*, 61, 4053-4065, 1997.

Mackensen, A., H.-W. Hubberten, T. Bickert, G. Fischer, and D. K. Fütterer, $\delta^{13}C$ in benthic foraminiferal tests of *Fontbotia wuellerstorfi* (Schwager) relative to $\delta^{13}C$ of dissolved inorganic carbon in Southern Ocean deep water: implications for Glacial ocean circulation models, *Paleoceanography, 8* (5), 587-610, 1993.

Martin, J.H. and G.A. Knauer, The elemental composition of plankton, *Geochim. Cosmochim. Acta*, 37, 1639-1653,1976.

McCorkle, D.C., P.A. Martin, D.W. Lea, and G.P. Klinkhammer, Evidence of a dissolution effect on benthic foraminiferal shell chemistry: $\delta^{13}C$, Cd/Ca, Ba/Ca, and Sr/Ca results from the Ontong Java Plateau, *Paleoceanography, 10* (4), 699-714, 1995.

Mook, W.G., Bommerson, J.C., Staverman, W.H., Carbon isotope fractionation between dissolved bicarbonate and gaseous carbon dioxide. *Earth Planet Sci. Lett.*, 22, 169-176, 1974.

Ninnemann, U.S., and C.D. Charles, Regional differences in Quaternary Subantarctic nutrient cycling: Link to intermediate and deep water ventilation, *Paleoceanography*, 12, 560-567, 1997.

Oppo, D.W., and R.G. Fairbanks, Variability in the deep and intermediate water circulation of the Atlantic during the past 25,000 years: Northern Hemisphere modulation of the Southern Ocean, *Earth Planet Sci. Lett.*, 86, 1-15, 1987.

Oppo, D.W., and S.J. Lehman, Mid-Depth Circulation of the Subpolar North Atlantic During the Last Glacial Maximum, *Science, 259,* 1148-1152, 1993.

Oppo, D.W., and Y. Rosenthal, Cd/Ca changes in a deep Cape Basin core over the past 730,000 years: Response of circumpolar deepwater variability to northern hemisphere ice sheet melting?, *Paleoceanography*, 9, 661-675, 1994.

Reid, J.L., W.D. Nowlin Jr., and W.C. Patzert, On the Characteristics and Circulation of the Southwestern Atlantic Ocean, *J. Phys. Oceanogr.*, 7, 62-91, 1977.

Rickaby, R.E.M., and H. Elderfield, Planktonic Cd/Ca: Paleonutrients or Paleotemperature?, Submitted to *Paleoceanography*, 1998.

Rosenthal, Y., Late Quaternary paleochemistry of the Southern Ocean: Evidence from cadmium variability in sediments and foraminifera. Ph.D. thesis, MIT/WHOI Joint Program, Cambridge, MA, 1994

Rosenthal, Y., P. Lam, E.A. Boyle, and J. Thomson, Authegenic cadmium enrichments in suboxic sediments: Precipitation and postdepositional mobility, *Earth Planet. Sci. Lett.*, 132, 99-111, 1995.

Rosenthal, Y., E.A. Boyle, and L. Labeyrie, Last glacial maximum paleochemistry and deepwater circulation in the Southern Ocean: Evidence from foraminiferal cadmium, *Paleoceanography,* 12, 787-796, 1997.

Shackleton, N.J., Carbon-13 in Uvigerina: Tropical rainforest history and the Equatorial Pacific carbonate dissolution cycles, in *The Fate of Fossil Fuel CO_2 in the Oceans*, edited by N.R. Andersen, and A. Malahoff, pp. 401-427, Plenum, New York, 1977.

Spero, H., I. Lerche, and D.F. Williams, Opening the carbon isotope "vital effect" black box, 2, Quantitative model for interpreting foraminiferal carbon isoptope data, *Paleoceanography*, 6, 639-655, 1991.

Spero, H.J. J. Bijma, D.W. Lea, and B.E. Bemis, Effect of seawater carbonate concentration on foraminiferal carbon and oxygen isotopes. *Nature,* 390, 497-500, 1997.

Yu, E.-F., M.P Bacon, and R. Francois, Similar rates of modern and last-glacial ocean thermohaline circulation inferred from radiochemical data, *Nature*, 379, 689-694, 1996.

Zahn, R., K. Winn and M. Sarnthein, Benthic foraminiferal $\delta^{13}C$ and accumulation rates of organic carbon: *Uvigerina Peregrina* group and *Cibicidoides Wuellerstorfi. Paleoceanography*, 1(1), 27-42, 1986.
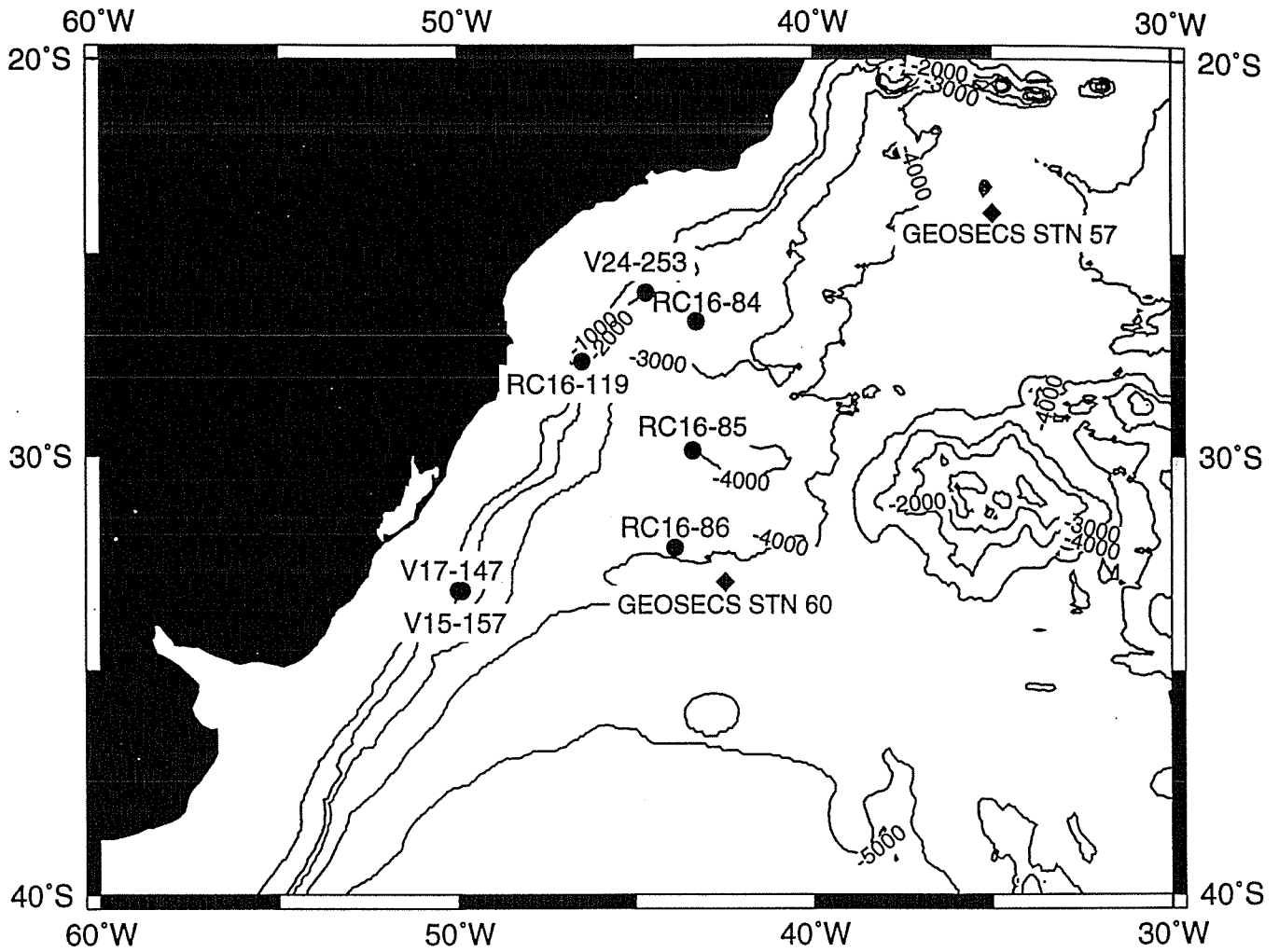
Fig. 1 A map of the study area with core locations and GEOSECS Stations.
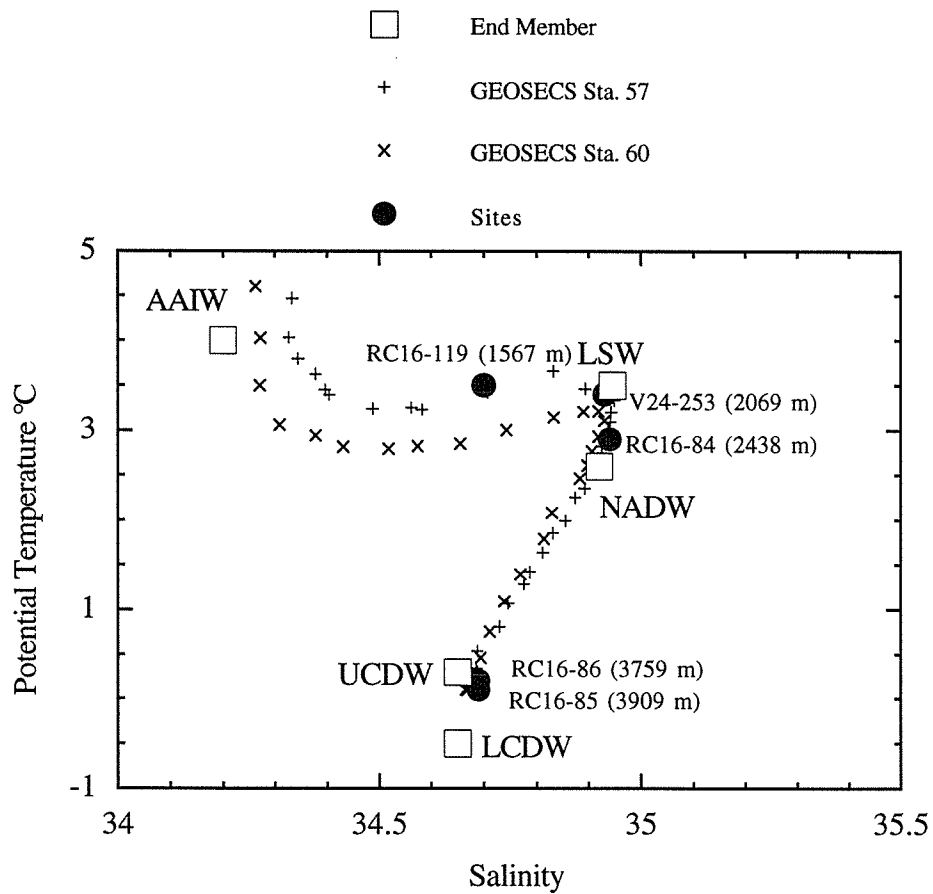
Figure 2. End member water masses, sites, and GEOSECS station data (Station 57; 23.98° S, 35.02° W and Station 60; 32.97° S 42.51° W) are plotted in salinity/potential temperature space.
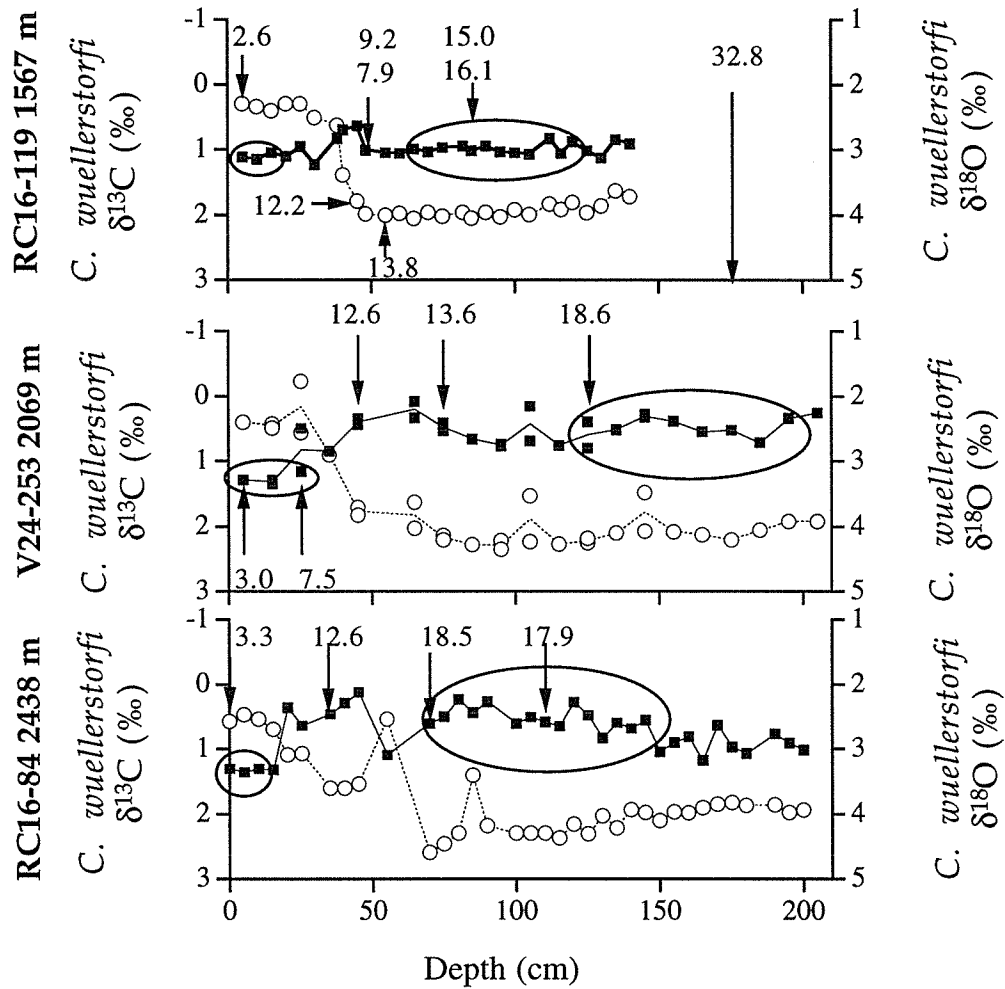
Figure 3. Stable benthic foraminiferal carbon (filled squares) and oxygen (open circles) isotopes are plotted. Radiocarbon ages are displayed. Data used in depth transects are circled.
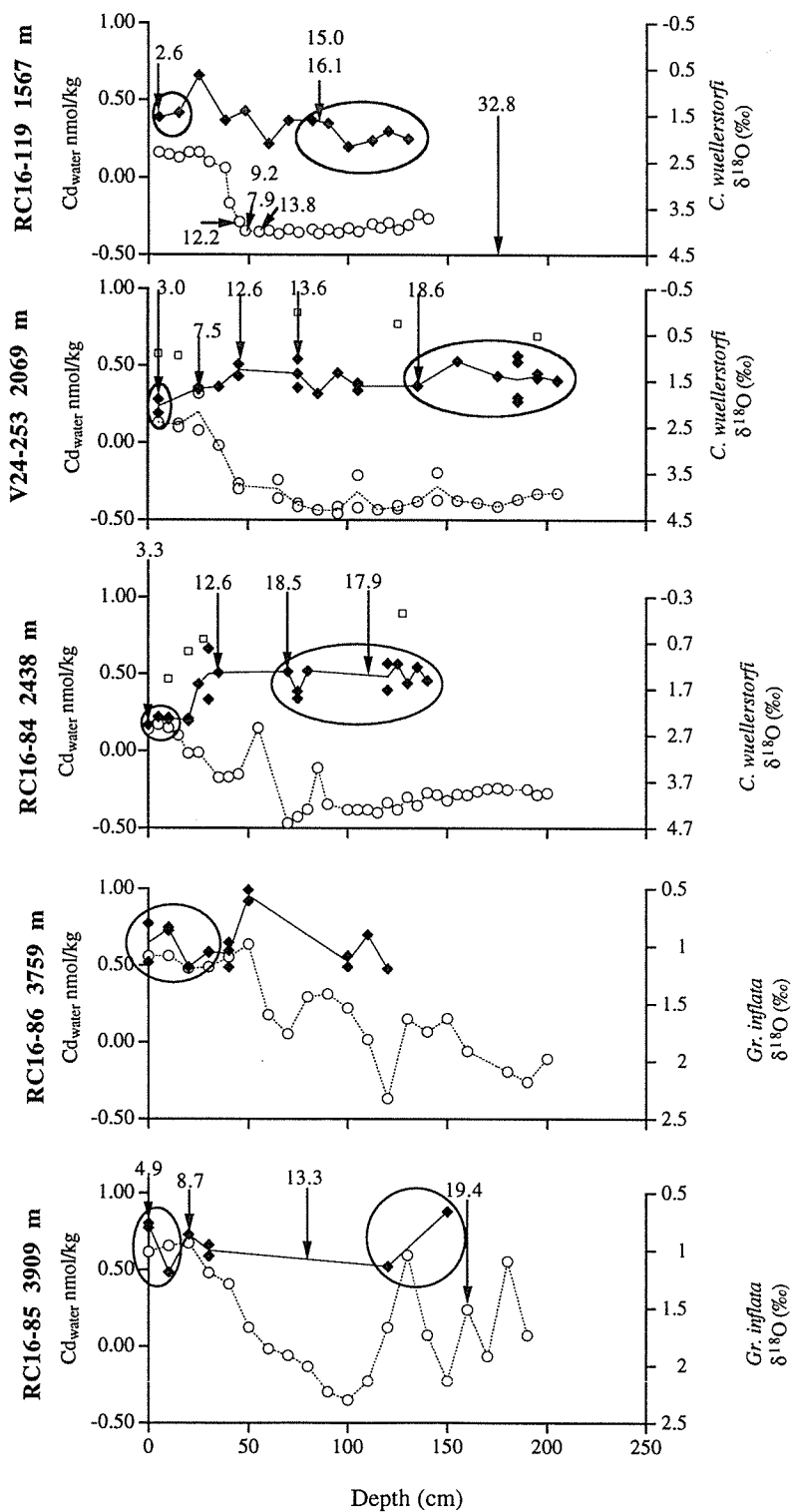
Figure 4. Benthic foraminiferal CdW estimates (solid symbols) plotted with oxygen isotope stratigraphies (open symbols) and radiocarbon ages. Data used in depth transects are circled. Cores are displayed by increasing water depth.
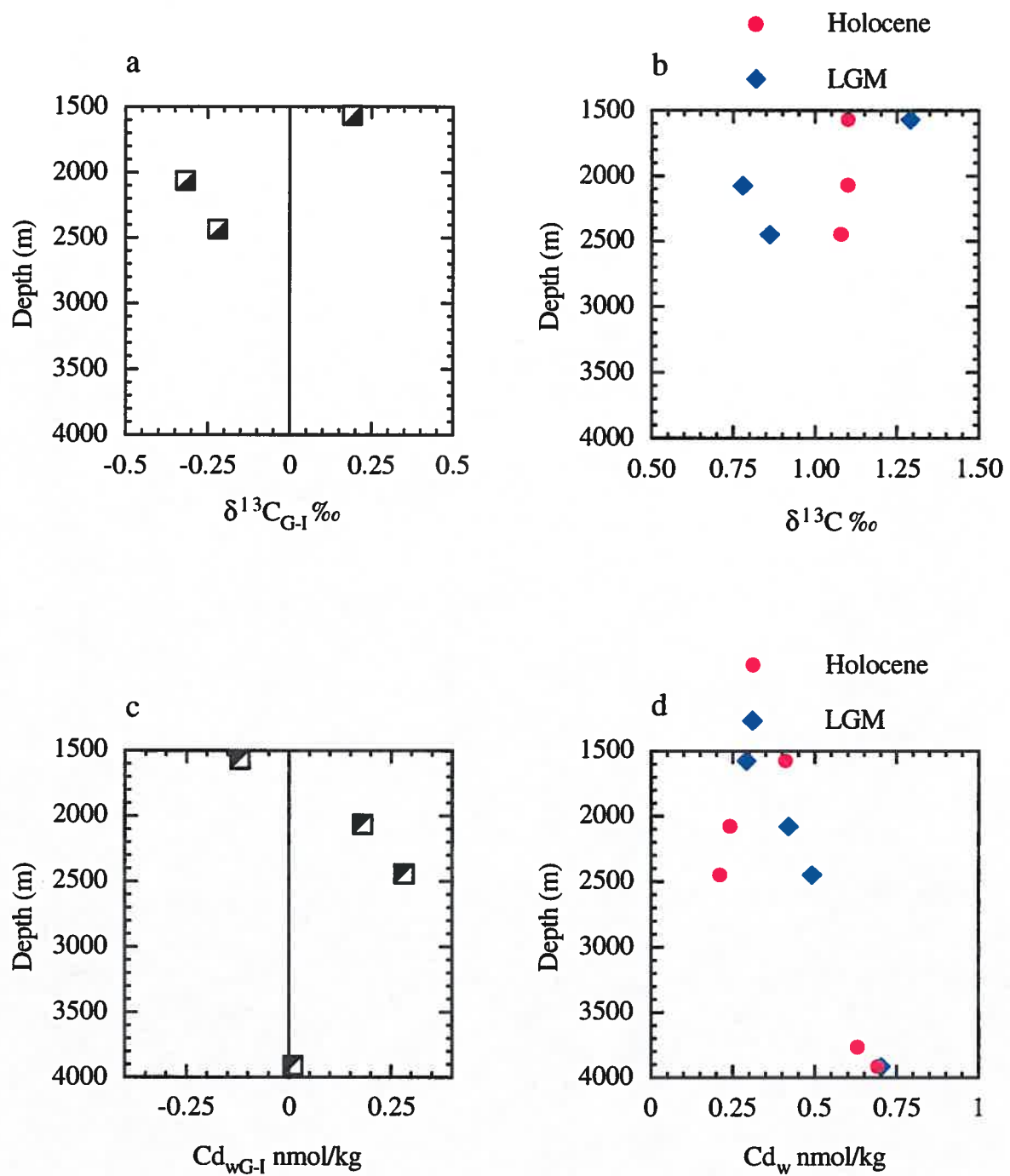
Figure 5. The glacial-interglacial differences in $\delta^{13}C$ (a), average Holocene and LGM $\delta^{13}C$ values (b), the glacial-interglacial difference in Cd_w (c), and average Holocene and LGM Cd_w estimates (d) suggest glacial nutrient depletion above 2000 m and increasing glacial nutrient content below that depth, with no change in the nutrient content of the deepest waters.
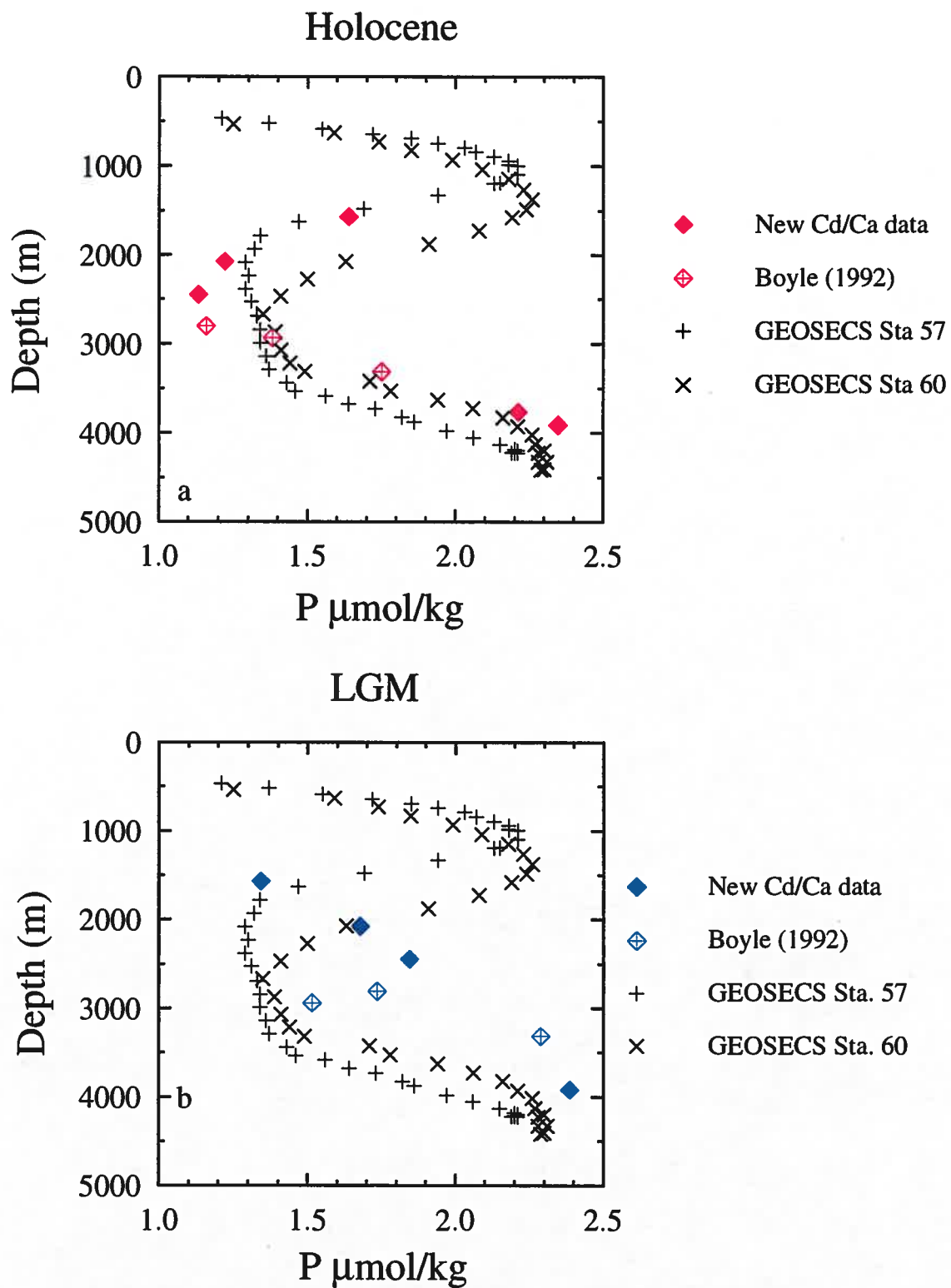
Figure 6. Holocene (a) and LGM (b) Cd/Ca estimates of phosphate compared to GEOSECS phosphate profiles from the western South Atlantic. The LGM Cd/Ca depth profile suggests a nutrient depleted water mass above 2000 m, and increasing nutrient content below that depth.

27
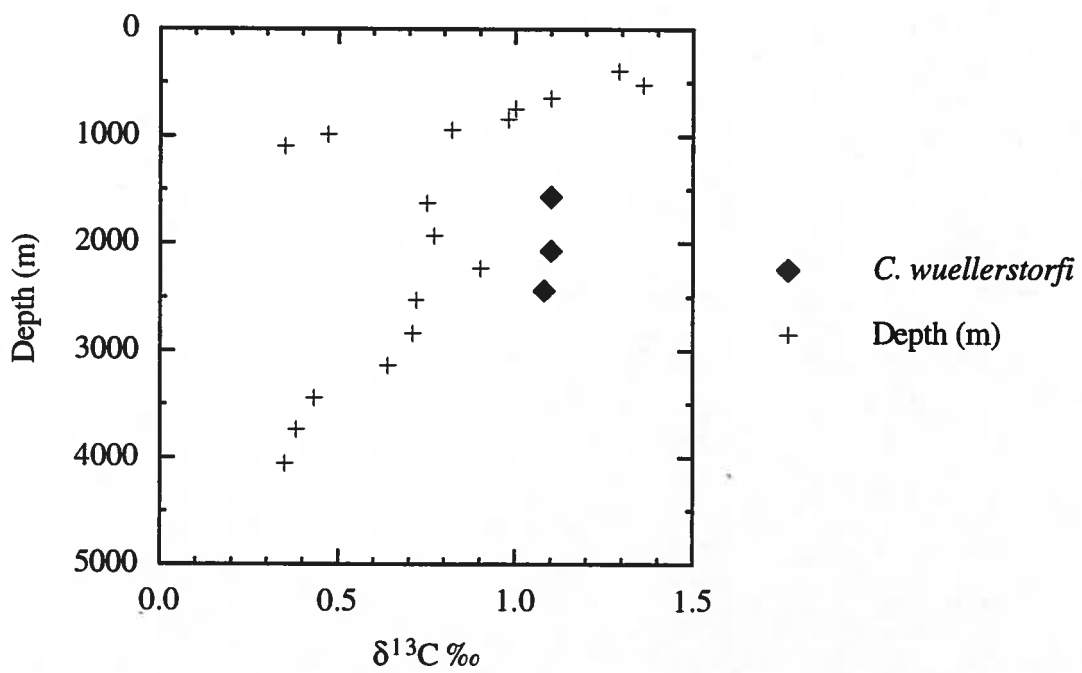
Figure 7. Benthic foraminiferal carbon isotope values are 0.3‰-0.4‰ higher than the nearest water column carbon isotope measurements (Kroopnick, 1985).
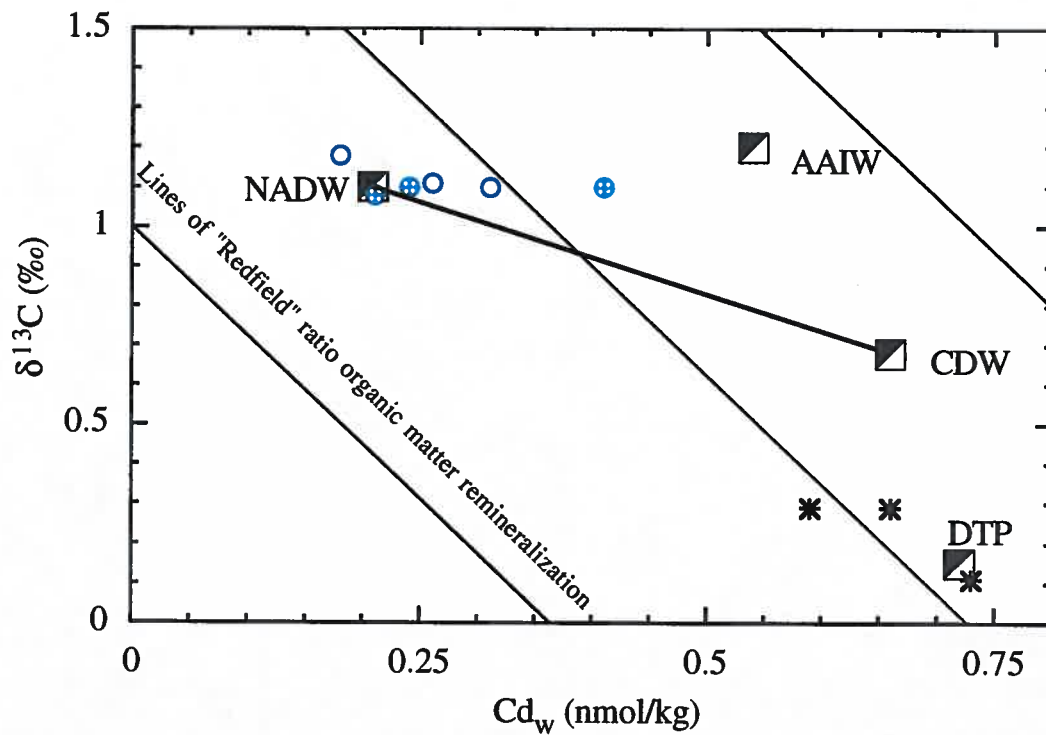
Figure 8. Western South Atlantic core top foraminiferal CdW values are plotted against foraminiferal carbon isotope values. End-member watermass compositions are derived from conversion of GEOSECS phosphate to an estimate of Cdw and from the carbon isotope measurments of Kroopnick (1985). Open circles denote western South Atlantic coretop data of Boyle (1992), crossed circles denote our new coretop western South Atlantic data, and stars denote Deep Tropical Pacific (DTP) coretop data of Boyle (1992). Lines of organic matter remineralization follow Broecker and Maier-Reimer (1992) and Lynch-Stieglitz et al. (1995,1996).
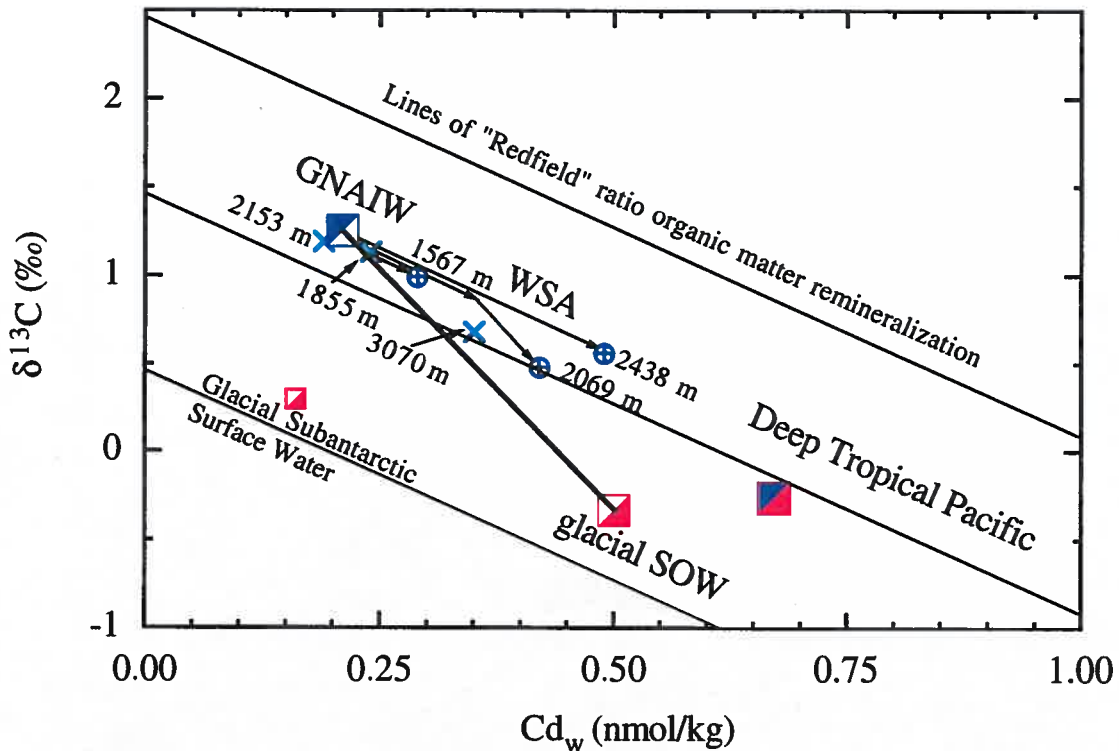
Figure 9. Glacial foraminiferal CdW values plotted against foraminiferal carbon isotope composition. The GNAIW, glacial SOW, and Deep Tropical Pacific end members are derived from Boyle (1992). The glacial Subantarctic surface water point is derived from the data of Rosenthal et al. (1997), Ninnemann and Charles (1997), and Rickaby and Elderfield (submitted manuscript, 1998). A mixing line connects GNAIW with glacial SOW. Western South Atlantic cores are plotted with blue crossed circles. Boyle's (1992) North Atlantic data from similar depths as our western South Atlantic data are plotted with cyan crosses. Lines of organic matter regeneration (Broecker and Maier-Reimer 1992; Lynch-Stieglitz et al., 1995,1996) cross the y-axis at arbitrarily differing preformed carbon isotope values. These lines assume a 0.3 ‰ lower glacial mean ocean carbon isotope composition (e.g. Duplessy et al., 1988; Curry et al., 1988, Boyle, 1992), 2‰ higher average glacial organic matter carbon isotope compostion (Rau et al., 1991), a 4 % increase in total inorganic carbon, and no change in the oceanic inventory of Cd (Boyle, 1992). Arrows show the approximate contributions of aging and mixing needed to yield western South Atlantic data.
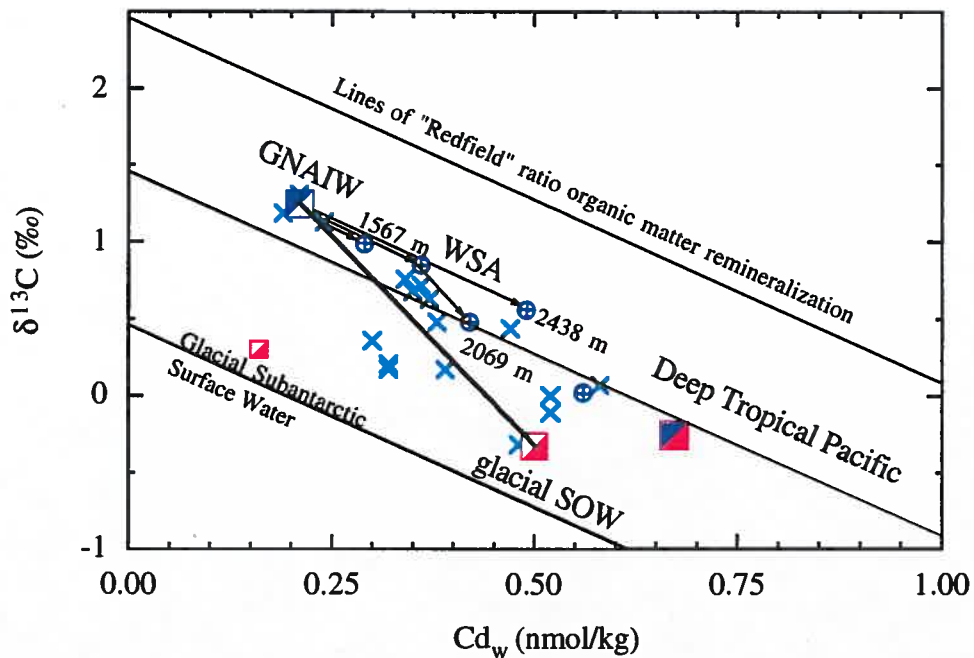
Figure 10. Glacial CdW values are plotted against foraminiferal carbon isotope composition as in Figure 9. Most of the open North Atlantic data (x) (Boyle, 1992) and new and published (Boyle, 1992) western South Atlantic data (blue crossed circles) can be described as an aged mixture of GNAIW and glacial SOW. Glacial Subantarctic surface water and glacial SOW had similar gas exchange signatures suggesting a Subantarctic source for glacial SOW. The pre-formed nutrient composition of the Deep Tropical Pacific falls between GNAIW and glacial SOW, but the Deep Tropical Pacific data falls far from the mixing line between GNAIW and glacial SOW along a line of organic matter remineralization. This implies that like today, deep Pacific waters were an aged mix of North and South Atlantic source waters during the LGM.

31

TABLES

Table 1: Core Locations

Core	Latitude	Longitude	Water depth (m)
RC16-119	27.70° S	46.517° W	1567
V24-253	26.95° S	44.683° W	2069
RC16-84	26.70° S	43.333° W	2438
RC16-86	32.17° S	43.933° W	3759
RC16-85	29.92° S	43.417° W	3909

Table 2: Endmember Properties

End Member Water Mass	°C	S (psu)	PO_4	$\delta^{13}C$[5]
Northern Component Water (NCW~NADW)[1,2]	2.6	34.92	1	1.1
Labrador Sea Water (LSW)[3]	3.5	34.95	1	1.1
Southern Component Water (SCW~LCDW)[1,2]	-0.5	34.65	2.3	0.68
Upper Circumpolar Deep Water (UCDW)[4]	0.3	34.65	2.3	0.68
Antarctic Intermediate Water (AAIW)[4]	4.0	34.2	2	1.1

1. Oppo and Fairbanks (1987)
2. Broecker et al. (1985)
3. Broecker and Peng (1982)
4. GEOSECS expedition
5. Kroopnick (1985)

Table 3: Modern Core Site Water Composition

Core	Depth m	Salinity (psu)	T °C	NCW %	CDW %	AAIW %
RC16-119	1567	34.70	3.5	65%$_{LSW}$	5%	30%
V24-253	2069	34.93	3.3	>95%$_{NADW}$	<5%	0%
RC16-84	2438	34.94	2.9	100%$_{NADW}$	0%	0%
RC16-86	3759	34.69	0.2	25%$_{NADW}$	75%	0%
RC16-85	3909	34.69	0.1	20%$_{NADW}$	80%	0%

Table 4: Oxygen and carbon isotope data

Core RC16-119	Water Depth (m) 1567	Foraminifera *C. wueller.*	Core V24-253	Water Depth (m) 2069	Foraminifera *C. wueller.*
Depth (cm)	$\delta^{18}O$	$\delta^{13}C$	Depth (cm)	$\delta^{18}O$	$\delta^{13}C$
5	2.29	1.11	5	2.394	1.282
10	2.33	1.14	15	2.421	1.285
15	2.4	1.04	15	2.489	1.337
20	2.29	1.1	25	1.766	0.49
25	2.29	0.95	25	2.56	1.151
30	2.5	1.22	35	2.891	0.844
38	2.62	0.82	45	3.707	0.341
40	3.38	0.69	45	3.821	0.43
45	3.78	0.63	65	3.628	0.075
48	3.98	1	65	4.022	0.327
55	4	1.04	75	4.131	0.406
60	3.97	1.05	75	4.199	0.525
65	4.05	0.98	85	4.276	0.652
70	3.95	1.03	95	4.206	0.735
75	4.01	0.96	95	4.347	0.764
82	3.95	0.94	105	3.529	0.152
85	4.04	1.01	105	4.224	0.681
90	3.95	0.94	115	4.265	0.751
95	4.02	1.03	125	4.248	0.388
100	3.92	1.04	125	4.172	0.799
105	3.99	1.06	135	4.099	0.514
112	3.83	0.82	145	3.474	0.271
116	3.91	1.05	145	4.071	0.321
120	3.8	0.87	155	4.075	0.379
125	3.96	1.01	165	4.125	0.54
130	3.85	1.12	175	4.205	0.518
135	3.62	0.84	185	4.054	0.71
140	3.71	0.9	195	3.921	0.336
			205	3.914	0.25

Core RC16-84	Water Depth (m) 2438	Foraminifera C. wueller		Core RC16-86	Water Depth (m) 3759	Foraminifera G. inflata
Depth (cm)	$\delta^{18}O$	$\delta^{13}C$		Depth (cm)	$\delta^{18}O$	
0	2.569	1.301		0	1.087	
5	2.461	1.355		10	1.081	
10	2.534	1.302		20	1.191	
15	2.691	1.318		30	1.18	
20	3.083	0.356		40	1.094	
25	3.066	0.636		50	0.982	
35	3.602	0.458		60	1.594	
40	3.597	0.285		70	1.76	
45	3.535	0.12		80	1.439	
55	2.536	1.088		90	1.415	
70	4.583	0.603		100	1.534	
75	4.453	0.498		110	1.811	
80	4.293	0.229		120	2.32	
85	3.4	0.436		130	1.63	
90	4.18	0.264		140	1.742	
100	4.294	0.603		150	1.626	
105	4.294	0.503		160	1.909	
110	4.296	0.58		180	2.087	
115	4.36	0.644		190	2.177	
120	4.149	0.271		200	1.974	
125	4.301	0.476				
130	4.028	0.829		Core RC16-85	Depth (m) 3909	Foraminifera G. inflata
135	4.212	0.591				
140	3.925	0.679		Depth (cm)	$\delta^{18}O$	
145	3.972	0.553		0	1.007	
150	4.101	1.038		10	0.953	
155	3.967	0.898		20	0.931	
160	3.979	0.808		30	1.187	
165	3.901	1.175		40	1.285	
170	3.849	0.628		50	1.664	
175	3.826	0.967		60	1.852	
180	3.867	1.068		70	1.909	
190	3.86	0.766		80	2.007	
195	3.974	0.907		90	2.226	
200	3.941	1.01		100	2.298	
				110	2.134	
				120	1.664	
				130	1.036	
				140	1.734	
				150	2.131	
				160	1.509	
				170	1.916	
				180	1.089	
				190	1.734	

Table 5:Radiocarbon Ages

Core	Depth (cm)	Radiocarbon Age (Kyr)*	Age error
V15-157	15	4.7	0.04
V15-157	35	8.6	0.06
V15-157	66	9.5	0.07
V17-147	4	2.6	0.06
V17-147	30	11.7	0.06
V17-147	50	6.8	0.04
V17-147	140	12.1	0.10
RC16-119	5	2.6	
RC16-119	45	12.2	
RC16-119	48	9.2	
RC16-119	48	7.9	
RC16-119	55	13.8	
RC16-119	85	16.1	
RC16-119	85	15.0	
RC16-119	175	32.8	
RC16-119	225	31.6	
RC16-119	275	40.5	
V24-253	5	3.1	0.04
V24-253	25	7.5	0.04
V24-253	45	12.7	0.07
V24-253	75	13.3	0.07
V24-253	125	18.7	0.10
RC16-84	0	3.3	0.03
RC16-84	35	12.6	0.07
RC16-84	70	18.6	0.15
RC16-84	115	18.0	0.12
RC16-84	200	31.5	0.21
RC16-85	0	4.9	0.04
RC16-85	20	8.7	0.08
RC16-85	70	13.3	0.16
RC16-85	160	19.5	0.20

*Not corrected for reservoir age.

Table 6: Cd/Ca data

Core	Latitude	Longitude	Water Depth (m)			
RC16-119	27.7° S	46.517° W	1567 m			

Sample Depth (cm)	[Cd] nmol/l	[Ca] µmol/ml	[Mn] µmol/l	Cd/Ca µmol/mol	Mn/Ca mmol/mol	Foraminiferal Species
5				0.064		C. wuellerstorfi
15				0.069		C. wuellerstorfi
25				0.110		C. wuellerstorfi
38				0.061		C. wuellerstorfi
48				0.072		C. wuellerstorfi
60				0.036		C. wuellerstorfi
70				0.061		C. wuellerstorfi
82				0.062		C. wuellerstorfi
90				0.058		C. wuellerstorfi
100				0.034		C. wuellerstorfi
112				0.040		C. wuellerstorfi
120				0.049		C. wuellerstorfi
130				0.042		C. wuellerstorfi

Core	Latitude	Longitude	Water Depth (m)			
V24-253	26.95° S	44.683° W	2069 m			

Sample Depth (cm)	[Cd] nmol/l	[Ca] µmol/ml	[Mn] µmol/l	Cd/Ca µmol/mol	Mn/Ca mmol/mol	Foraminiferal Species
5	0.561	13.970	0.087	0.040	0.006	Cibicidoides sp.
5	0.806	13.624	0.147	0.059	0.011	C. wuellerstorfi
5	1.088	18.703	0.000	0.058	0.000	H. elegans
15	1.594	28.126	0.001	0.057	0.000	H. elegans
25	0.878	11.675	0.190	0.075	0.016	C. kullenbergi
25	2.293	31.612	0.441	0.073	0.014	Cibicidiodes sp.
35	1.736	22.816	0.770	0.076	0.034	C. wuellerstorfi
45	2.188	24.125	0.756	0.091	0.031	Uvigerina sp.
45	1.168	10.929	0.806	0.107	0.074	C. kullenbergi
75	1.415	15.042	0.471	0.094	0.031	Uvigerina sp.
75	0.447	5.947	0.520	0.075	0.088	C. wuellerstorfi
75	1.669	19.644	0.013	0.085	0.001	H. elegans
75	2.575	22.538	1.005	0.114	0.045	Uvigerina sp.
85	2.012	29.989	1.648	0.067	0.055	C. wuellerstorfi
95	1.712	17.979	0.358	0.095	0.020	Uvigerina sp.
105	0.791	9.993	1.050	0.079	0.105	C. wuellerstorfi
105	1.700	23.780	2.687	0.071	0.113	C. wuellerstorfi
105	0.574	7.058	0.169	0.081	0.024	Uvigerina sp.
125	0.779	2.122	0.064	0.367	0.030	Uvigerina sp.
125	0.855	11.027	0.000	0.078	0.000	H. elegans
135	0.964	12.410	0.482	0.078	0.039	Uvigerina sp.
135	0.771	9.978	1.356	0.077	0.136	C. wuellerstorfi
145	0.530	4.466	1.181	0.119	0.264	C. wuellerstorfi

Core V24-253	Latitude 26.95° S	Longitude 44.683° W	Depth 2069 m			
Sample Depth (cm)	[Cd] nmol/l	[Ca] µmol/ml	[Mn] µmol/l	Cd/Ca µmol/mol	Mn/Ca mmol/mol	Foraminiferal Species
145	*2.106*	*8.742*	*0.525*	***0.241***	*0.060*	Uvigerina sp.
155	2.105	18.950	1.055	0.111	0.056	Uvigerina sp.
175	*1.635*	*8.161*	*3.122*	*0.200*	***0.383***	C. wuellerstorfi
175	0.827	9.079	0.279	0.091	0.031	Uvigerina sp.
185	3.775	34.270	1.989	0.110	0.058	Uvigerina sp.
185	3.708	31.199	0.749	0.119	0.024	Uvigerina sp.
185	1.067	18.953	2.130	0.056	0.112	C. wuellerstorfi
185	1.052	17.094	1.664	0.062	0.097	C. wuellerstorfi
185	1.258	23.652	0.006	0.053	0.000	H. elegans
195	0.820	9.302	0.593	0.088	0.064	Uvigerina sp.
195	2.247	23.810	1.759	0.094	0.074	Uvigerina sp.
195	0.942	13.547	0.042	0.070	0.003	H. elegans
195	*1.077*	*10.805*	*2.315*	*0.100*	***0.214***	C. wuellerstorfi
205	1.282	15.079	0.510	0.085	0.034	C. kullenbergi
205	2.201	26.040	1.374	0.085	0.053	Uvigerina sp.

Core RC16-84	Latitude 26.7° S	Longitude 43.333° W	Water Depth (m) 2438 m			
Sample Depth (cm)	[Cd] nmol/l	[Ca] µmol/ml	[Mn] µmol/l	Cd/Ca µmol/mol	Mn/Ca mmol/mol	Foraminiferal Species
0.0	0.607	14.823	0.232	0.041	0.016	Cibicidoides sp.
5.0	1.133	21.223	0.089	0.053	0.004	mixed Cibicidoides sp.
10.0	1.062	20.484	0.103	0.052	0.005	C. kullenbergi
10.0	0.964	19.648	0.203	0.049	0.010	Cibicidoides sp.
10.0	0.856	18.262	0.012	0.047	0.001	H. elegans
20.0	1.093	21.569	0.249	0.051	0.012	C. wuellerstorfi
20.0	1.003	21.279	0.070	0.047	0.003	C. kullenbergi
20.0	1.480	22.830	0.013	0.065	0.001	H. elegans
25.0	2.251	21.515	0.153	0.105	0.007	C. kullenbergi
27.5	1.867	25.656	0.000	0.073	0.000	H. elegans
30.0	2.383	14.840	0.043	0.161	0.003	C. kullenbergi
30.0	1.531	18.995	0.362	0.081	0.019	Cibicidoides sp.
35.0	2.932	23.905	0.260	0.123	0.011	C. wuellerstorfi
70.0	0.844	6.781	0.474	0.124	0.070	Uvigerina sp.
75.0	0.786	9.542	0.614	0.082	0.064	Uvigerina sp.
75.0	1.848	19.770	1.010	0.093	0.051	Uvigerina sp.
75.0	*1.945*	*16.794*	*2.800*	*0.116*	***0.167***	C. wuellerstorfi
80.0	1.534	12.203	0.425	0.126	0.035	Uvigerina sp.
110.0	*3.227*	*18.492*	*2.802*	*0.174*	***0.152***	C. wuellerstorfi
120.0	0.737	7.707	0.899	0.096	0.117	C. wuellerstorfi
120.0	3.346	24.417	1.009	0.137	0.041	Uvigerina sp.
125.0	*0.776*	*5.447*	*1.290*	*0.142*	***0.237***	C. wuellerstorfi
125.0	3.060	22.454	1.070	0.136	0.048	Uvigerina sp.

Core RC16-84	Latitude 26.7° S	Longitude 43.333° W	Depth 2438 m			
Sample Depth cm	[Cd] nmol/l	[Ca] µmol/ml	[Mn] µmol/l	Cd/Ca µmol/mol	Mn/Ca mmol/mol	Foraminiferal Species
127.5	1.198	13.380	0.046	0.090	0.003	H. elegans
130.0	1.064	10.050	0.344	0.106	0.034	Cibicidoides sp.
135.0	2.468	18.759	1.029	0.132	0.055	Uvigerina sp.
140.0	1.107	10.027	0.471	0.110	0.047	Uvigerina sp.
140.0	*0.810*	*8.741*	*1.560*	*0.093*	***0.179***	*C. wuellerstorfi*

Core RC16-86	Latitude 32.2° S	Longitude 43.9° W	Water Depth (m) 3759 m			
Sample Depth cm	[Cd] nmol/l	[Ca] µmol/ml	[Mn] µmol/l	Cd/Ca µmol/mol	Mn/Ca mmol/mol	Foraminiferal Species
0	4.209	27.805	1.229	0.151	0.044	C. wuellerstorfi
0	4.458	19.832	0.229	0.225	0.012	Uvigerina sp.
10	3.340	15.820	0.191	0.211	0.012	Uvigerina sp.
10	3.225	14.845	1.786	0.217	0.120	Mixed benthics
20	4.832	33.897	1.451	0.143	0.043	Uvigerina sp.
30	2.275	13.287	1.423	0.171	0.107	C. wuellerstorfi
30	5.309	31.245	1.804	0.170	0.058	Uvigerina sp.
40	4.271	24.624	1.543	0.173	0.063	C. wuellerstorfi
40	4.320	30.402	3.089	0.142	0.102	C. wuellerstorfi
40	4.097	21.721	0.884	0.189	0.041	Uvigerina sp.
50	9.275	32.194	0.998	0.288	0.031	C. wuellerstorfi
50	3.232	12.123	0.427	0.267	0.035	Uvigerina sp.
100	4.930	34.526	0.524	0.143	0.015	Uvigerina sp.
100	2.332	14.297	1.351	0.163	0.094	C. wuellerstorfi
110	4.096	20.165	1.758	0.203	0.087	Mixed benthics
120	2.249	16.183	0.218	0.139	0.013	C. wuellerstorfi

Core RC16-85	Latitude 29.9° S	Longitude 43.4° W	Water Depth (m) 3909 m			
Sample Depth cm	[Cd] nmol/l	[Ca] µmol/ml	[Mn] µmol/l	Cd/Ca µmol/mol	Mn/Ca mmol/mol	Foraminiferal Species
0.0	5.732	24.587	0.092	0.233	0.004	Cibicidoides sp.
0.0	5.361	23.865	0.020	0.225	0.001	Melonis pompiloides
10.0	2.070	14.683	0.050	0.141	0.003	N. umbonifera
20.0	2.538	11.964	0.044	0.212	0.004	C. wuel & N. umbonif
30.0	4.009	23.335	0.268	0.172	0.011	C. wuellerstorfi
30.0	4.193	21.766	0.074	0.193	0.003	N. umbonifera
87.5	*4.321*	*16.228*	*2.950*	*0.266*	***0.182***	*Mixed benthics*
105.0	*4.973*	*18.453*	*4.156*	*0.269*	***0.225***	*2 Cib sp., 5 N. umbon.*
120.0	2.631	17.276	1.922	0.152	0.111	C. wuellerstorfi
150.0	0.936	3.659	0.353	0.256	0.096	Cibicidoides sp.
160.0	*3.019*	*14.763*	*8.432*	*0.205*	***0.571***	*C. wuellerstorfi*
160.0	*1.613*	*8.153*	*5.060*	*0.198*	***0.621***	*N. umbonifera*
160.0	*2.169*	*10.406*	*3.965*	*0.208*	***0.381***	*Exigua*
170.0	*2.215*	*12.635*	*2.510*	*0.175*	***0.199***	*Exigua/N. Umbonifera*

*Rejected analyses are in italics. The basis for rejection is displayed in bold.

Table 7: Glacial-Interglacial Nutrient Change

Site	Depth (m)	Holocene CdW$_{foram}$ nmol/kg	Holocene $\delta^{13}C$ (‰)	LGM CdW$_{foram}$ nmol/kg	LGM $\delta^{13}C$ (‰)	Cdw$_{G-I}$ nmol/kg	$\delta^{13}C_{G-I}$ (‰)**	ΔPO_4 Cd/Ca predicted	ΔPO_4 $\delta^{13}C$ predicted
RC16-119	1567	0.41	1.1	0.29	0.99	-0.12	0.19	-0.30	-0.17
V24-253	2069	0.24	1.1	0.42	0.48	0.18	-0.32	0.45	0.29
RC16-84	2438	0.21	1.08	0.49	0.56	0.28	-0.22	0.70	0.20
RC16-86	3759	0.63		0.59		-0.04		-0.1	
RC16-85	3909	0.69		0.70		0.01		0	

**A constant of 0.3‰ has been added to LGM $\delta^{13}C$ data to account for mean ocean $\delta^{13}C$ change

Table 8: Watermass Composition from T&S and Foraminiferal measurements

Site	Depth (m)	NADW TS/Foram	AAIW TS/Foram	CDW TS/Foram
RC16-119	1567	65%/45%	30%/45%	5%/10%
V24-253	2069	>95%/92%	0%/7%	<5%/2%
RC16-84	2438	100%/100%	0%/0%	0%/0%